doi:10.1115/ICEF2018-9691 Pre-Print

Proceedings of the ASME 2018 Internal Combustion Fall Technical Conference
ICEF2018
November 4-7, 2018, San Diego, CA, USA

INVESTIGATION OF THE EFFECT OF ELECTRODE SURFACE ROUGHNESS ON SPARK IGNITION

Mohammadrasool Morovatiyan
Dept. of Mechanical Engineering
University of Massachusetts Lowell
Lowell, MA, USA

Martia Shahsavan
Dept. of Mechanical Engineering
University of Massachusetts Lowell
Lowell, MA, USA

Mengyan Shen
Dept. of Physics & Applied Physics
University of Massachusetts Lowell
Lowell, MA, USA

J. Hunter Mack
Dept. of Mechanical Engineering
University of Massachusetts Lowell
Lowell, MA, USA

ABSTRACT

Lean-burn engines are important due to their ability to reduce emissions, increase fuel efficiency, and mitigate engine knock. In this study, the surface roughness of spark plug electrodes is investigated as a potential avenue to extend the lean flammability limit of natural gas. A nano-/micro-morphology modification is applied on surface of the spark plug electrode to increase its surface roughness. High-speed Z-type Schlieren visualization is used to investigate the effect of the electrode surface roughness on the spark ignition process in a premixed methane-air charge at different lean equivalence ratios. In order to observe the onset of ignition and flame kernel behavior, experiments were conducted in an optically accessible constant volume combustion chamber at ambient pressures and temperatures. The results indicate that the lean flammability limit of spark-ignited methane can be lowered by modulating the surface roughness of the spark plug electrode.

KEYWORDS
Constant Volume Combustion Chamber, Premixed Combustion, Spark plug electrode surface roughness, Flammability Limit, Lean-Burn Engines, Natural Gas

INTRODUCTION

The combustion of fossil and renewable fuels plays a critical role in the production of energy across the world. The consumption of these fuels gives rise to several concerns, including emissions, efficiency, and performance. To address these concerns, combustion systems have evolved over time, implementing a wide variety of approaches. Fuels are broadly utilized in premixed [1-4] and non-premixed combustion [5-9] using gas turbines and different forms of internal combustion (IC) engines such as spark ignition (SI) [10-12], homogeneous charge compression ignition (HCCI) [13-15], and reactivity controlled compression ignition (RCCI) [16, 17]. Natural gas, as one of the cleanest fossil fuels, is one of the main sources of energy production and electricity generation in the United States and abroad. Therefore, many studies have been done to investigate the effect of different operating conditions such as temperature, pressure, and equivalence ratio (from lean to rich).

Ignition in a combustible mixture is defined as a heat transfer process that is initiated at a longer time in comparison with the time for an electrical breakdown of the mixture between the electrodes [18]. There are various studies about different types of ignition systems such as spark ignition (SI) [11], compression ignition (CI) [19], plasma ignition [20], and microwave-assisted ignition [21] to ignite the combustible mixture for the purpose of converting chemical energy to mechanical energy. SI engines typically utilize an external heat source (e.g. spark plug) to ignite the mixture in the cylinders. CI engines typically operate with mechanical compression to elevate the mixture temperature, which provides the required condition to ignite the mixture and produce work. Plasma ignition uses high energy plasma to deliver the minimum ignition energy needed for ignition onset of a combustible mixture.

The spark ignition is initiated with a spark using an external heat origin like a spark plug to perform as an ignitor. The composition of a spark needs an avalanche of electrons discharged between electrodes. According to Townsend theory, a large swift supply of electrons produces fresh ions and electrons that leads to a transient discharge [22]. If the discharge that happens from cathode (positive terminal) to anode (negative terminal) has enough energy to ionize gas, the electrode gap is bridged to make a transition between ionized gases from a weaker to a stronger. This transition is typically called with spark and the area between the electrodes is considered as spark channel. According to the earlier studies, the spark discharge is dependent on several factors such as the electrode gap length, electrode shape, its material, gas pressure, the applied voltage and the discharge circuit [18, 22]. This study examines another effective factor on the discharge that has not been previously studied.

Spark-ignited engines are heavily utilized, especially in transportation systems. Therefore, it is crucial to enhance their efficiency along with reducing their emissions. Ignition systems in SI engines effectively play a key role in boosting mechanical performance and thermal efficiency. Several studies have investigated spark plug design to examine the factors affecting ignition, including spark plug gap size [23], electrode size and geometry [24], and number of ground electrodes [25]. Badawy et al [23] compared the effects of three different spark plug gaps on flame kernel growth and demonstrated that larger gap sizes lead to larger flame kernel regions. They also mentioned that the impact of the spark plug gap size is significant only at lean and stoichiometric conditions. The smaller gap sizes generate lower engine load output, along with lower in-cylinder pressure, heat release rate, and flame speed. Bane, Ziegler, and Shepherd [24] studied the effects of three different electrode geometries on flame onset, spark kernel, and flame formation. Spark kernel is effectively influenced by the electrode geometry, which generally leads to a spherical structure in vicinity of the electrode surfaces and cylindrical near the center of spark gap.

Lean combustion has gained a clear interest in several applications due to its significant benefits on fuel economy, environment pollution, and engine performance. Lean conditions have a potential capability to reduce emissions, increase fuel efficiency [26], improve thermal efficiency [27], and mitigate engine knock [28]. A lean mixture is provided with higher oxygen concentration compared to a stoichiometric mixture. This leads engines to have excess oxygen to burn an amount of fuel. Theoretically, since the fuel is consumed completely in the lean conditions, hydrocarbon emissions are reduced. Lean conditions also play a key role with respect to fuel economy. The ideal thermal efficiency of an IC engine (Equation 1), which is strongly dependent on the ratio of the specific heats of the mixture, can be boosted in leaner conditions due to the higher ratios of the specific heats for the leaner mixture. This ratio for the mixture would be larger while increasing the excess air.

$$\eta = 1 - \left(\frac{1}{r^{(\gamma-1)}}\right) \tag{1}$$

In this study, experiments have been conducted with a high-speed Z-type Schlieren system to investigate the effect of spark plug electrode surface roughness as a potential avenue to extend the lean flammability limit of natural gas. A constant volume combustion chamber (CVCC) filled by a premixed methane-air mixture with different lean equivalence ratios was used to study the electrode surface roughness on spark ignition. An electrode surface modification is implemented using femtosecond laser pulses to increase the surface roughness. Then, the effect of raw spark plug with no surface modification is compared to the nanostructured spark plug to assess the onset of ignition and flame kernel behavior.

METHODS

Experimental Setup

Experiments were conducted in an optical constant volume combustion chamber (CVCC), shown in Figure 1, to visually study effect of spark plug electrode surface roughness on flame kernel growth, flame morphology and its instability. The optical CVCC is a cylindrical chamber with an internal diameter and length of 140 mm. The chamber is built from stainless steel and equipped with two flanges at both ends to support two 50.8 mm thick fused quartz windows. The cylindrical optical CVCC and flanges are sealed to the quartz windows with nitrile rubber elastomer O-rings. The chamber contains a high precision piezoelectric pressure transducer (KISTLER 601CAA), a thermocouple (OMEGA KMTXL-062G-6), a gas inlet/outlet, and a spark plug. In order to observe the flame development, a Z-type Schlieren ensemble is employed using a high-speed high-resolution CMOS camera (Edgertronic SC2+), two concave mirrors, a light source with a pin hole, and a knife edge. The high-speed CMOS camera has a capture rate of up to 31,191 frames per second whose capture rate and shutter speed is optimized depending on the flame burning speed and the brightness of the flame front. In this setup, the light source and the knife edge is supported at the focal length of the mirrors which is 1524 mm. Figure 2 displays a schematic diagram of the experimental ensemble including the gas delivery system, pressure control units, ignition system, Z-type Schlieren arrangement, and data acquisition.

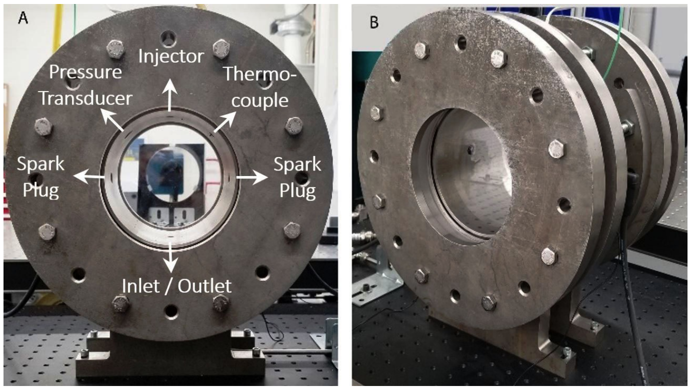

Figure 1. Optical constant volume combustion chamber in (A) Side view, (B) Isometric View

A wide range of lean equivalence ratios was performed to study lean flammability limit (LFL) of methane (as the primary component of natural gas) for both spark plugs with different surface roughness. Initial pressure and temperature for all cases were kept constant on 1 bar and 25 degrees Celsius, respectively. The methane-air mixture is ignited in the CVCC by a conventional ignition, operating with a coil, a DC power supply, and a capacitor. The ignition system utilizes a primary and secondary circuit to provide high voltage for the spark plug electrode that enables the spark plug to ionize the gaseous mixture in a spark channel created between the spark plug electrodes. If this voltage is high enough to pass the breakdown voltage, the spark gap functions as a bridge with Townsend avalanche of electrons discharging from cathode (positive terminal) to anode (negative terminal) [22].

Nano-/Micro-Morphology Modifications

There are several methods to fabricate nanometer-scale and micrometer-scale structures on solid substrates. One prominent technique is to make these structures on metallic surfaces employs ultra-short pulse lasers [29]. The femtosecond pulsed laser irradiates electromagnetic pulses in a very short time duration on the order of a femtosecond. The fabrication procedure exposes the solid surface to the femtosecond laser beam by scanning the substrate line by line across the surface. These pulses have the potential to irreversibly change the surface of metals by creating either nanostructures or microstructures on their substrate. Due to the scanning, the surface temperature possibly passes the melting point, and silicone oil is applied on the surface of the solid to decrease the possibility of damage and prevent surface oxidation. Irradiating the electrode surface with femtosecond laser pulses above the ablation threshold develops the ripple substrates on the electrode surface. This approach is a roughness-enhanced method, which effectively roughens electrode surface and adds conducting protrusions at the surface.

The process was carried out on spark plug (BOSCH WR8LC+) electrodes by bending its ground electrode to make the electrode accessible for the laser beams. We then bend the ground electrode back to its primary situation keeping the

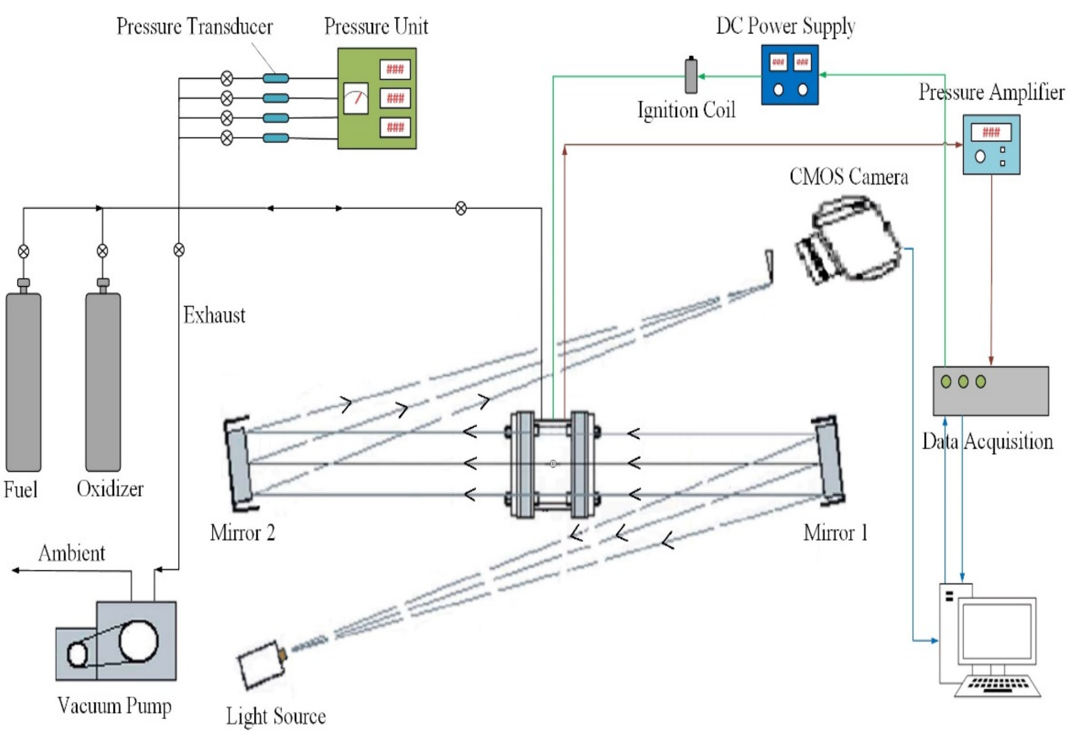

Figure 2. Schematic diagram of experimental systems

electrode gap constant that is 1 mm. To observe the surface modification with femtosecond laser pulses, a destructive testing method was required. The electrodes were removed from the spark plugs to make them fitted for material characterization devices using a Scanning Electron Microscope (SEM). Figure 3 shows the effect of laser spot scanning on forming the rippled nano-/micro-structures on the surface of the electrode. A Wyko NT2000 Optical Profiler has been used to measure the root mean square (RMS) surface roughness for the raw spark plug and exposed spark plug that were 3.37 μm and 4.93 μm, respectively. This indicates a 46.3% increase in surface roughness due to the fabrication procedure.

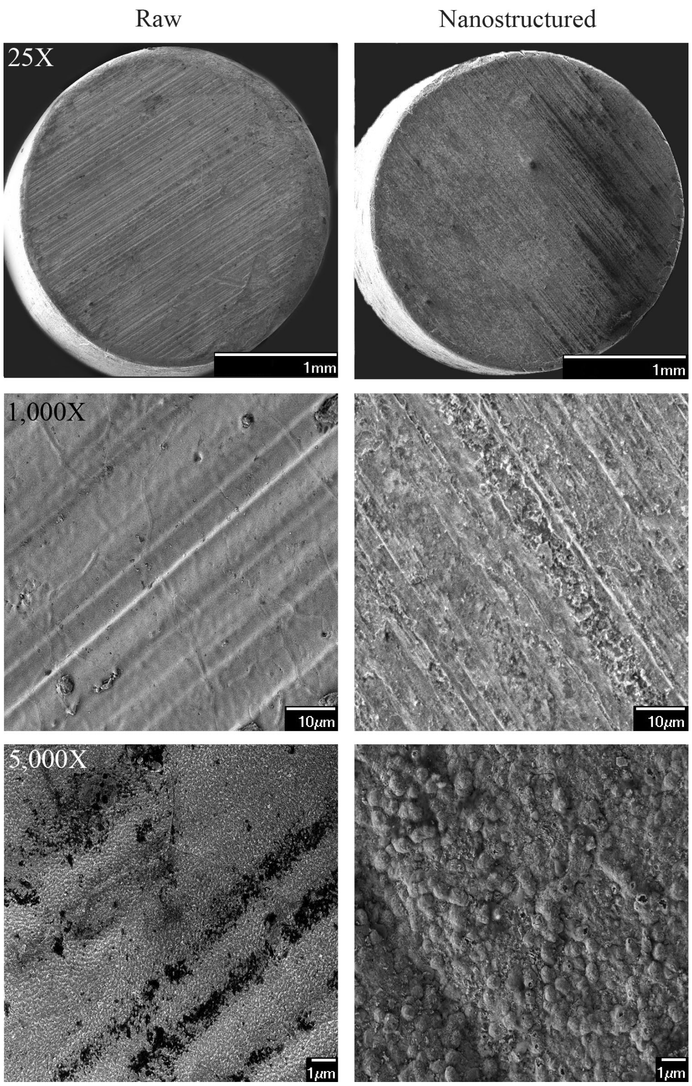

Figure 3. Scanning Electron Microscope images of the electrode surface with different magnification rates

RESULTS AND DISCUSSION

Surface roughness and breakdown voltage

According to the earlier studies, the correlation between electrode surface roughness and breakdown voltage has been theoretically and experimentally quantified [30, 31]. Sato et al studied an electrode made of copper, the same as the electrode material of the spark plugs performed in this study. Equation 2 describes a simple general relationship between breakdown voltage and electrode surface roughness [31]:

$$V_{50} = AR^{-n} \quad (2)$$

Where V_{50} is 50% breakdown voltage, R is defined as centerline average roughness (ISO 468-1982 and ISO 4284/1-1984), and A and n are constants formulated as a function of gap length.

This formula indicates that increasing electrode surface roughness exponentially decreases the breakdown voltage. Therefore, nanostructures produced by femtosecond laser pulses potentially decrease the breakdown voltage and lessens the onset electrical field strength [30]. This may be implied that the higher roughness provides a lower minimum ignition energy that is required to ignite the gaseous mixture.

Lean flammability limit

The impact of electrode surface roughness on the lean flammability limit (LFL) was studied using a methane-air mixture ignited by both spark plugs. The experiment has been repeated four times for each equivalence ratio by each spark plugs to study its accuracy and repeatability. The uncertainty of equivalence ratio is ±0.6% and of maximum pressure is ±0.1 bar. The results indicate that roughening the electrode surface plays a role in decreasing the LFL. According to the previous studies, the LFL of methane-air mixture has been reported near 5% [32, 33]. Figure 4 shows the maximum pressure of premixed methane-air combustion along different equivalence ratios for both spark plugs. These results indicate that the nanostructured spark plugs have a lower LFL compared to the raw spark plug. In addition, its minimum LFL reaches 5.9% (equivalence ratio is 0.57), however, the purity of methane gas is an important factor on flammability limit that needs to be considered. This enhancement on lean flammability limit may be due to a lower minimum ignition energy and higher heat transfer, both of which contribute to ignition onset [18]. In further studies, high-precision thermistor sensors can be employed to accurately determine the temperature at each electrode.

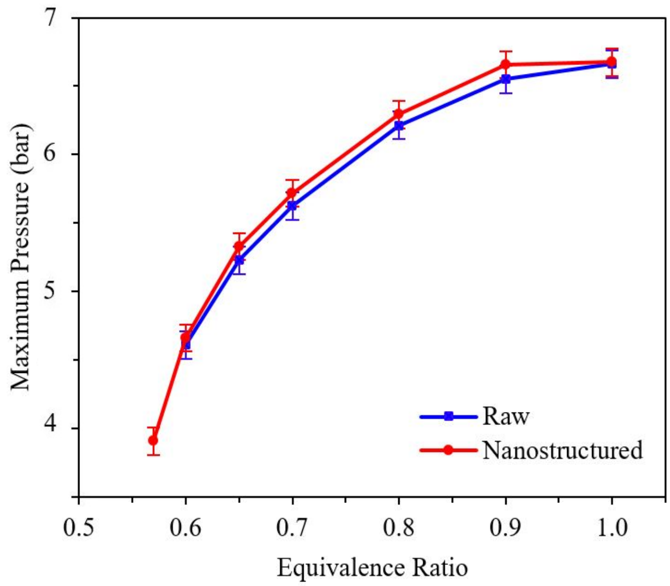

Figure 4. Maximum pressure of combustion along different equivalence ratios for both spark plugs

Image Analysis

Figure 5 shows the flame propagation of the spark-ignited methane-air mixture through the optical cylindrical CVCC for several time frames. The images visually display that the flame development is almost identical for both spark plugs with different electrode surface roughnesses. According to this preliminary study, the major difference between them is related to flame stability, which is seen in the middle frames. As shown, in the case of the raw spark plug, the flame front becomes instable, and cellular flames appear with different patterns. On the other hand, in case of the nanostructured spark plug, the flame front propagates through the mixture much more smoothly in the laminar state and is much stable with fewer flame cells, possibly due to delivering a lower electric field strength from the nanostructured spark plug. This can possibly imply that manipulating the electrode surface roughness leads to stable flames compared to the smoother electrode surface.

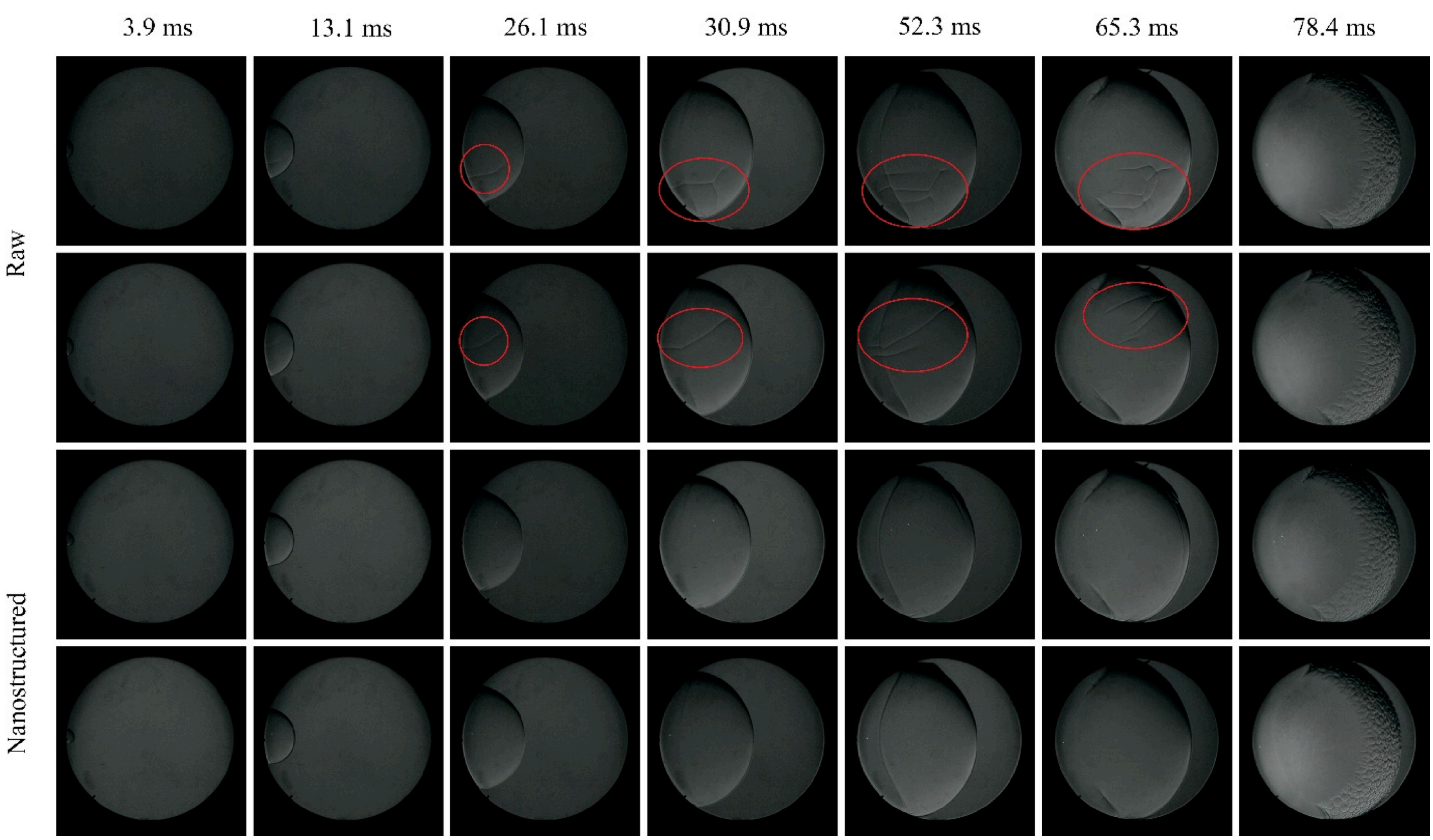

Figure 5. Flame kernel development in the premixed combustion of methane -air mixture for several time frames

Apart from the irregular flame patterns seen in the middle frames by ignition of the raw spark plug, both flame fronts became unstable near the walls as expected. This wrinkled flame morphology is due to turbulence, which caused by the interface between the burned gas and the unburned gas happened at a very short time scale, distorting the laminar flame front [34]. The laminar flame thickness is smaller or equal to Kolmogorov microscale in the wrinkled flame region.

If the early stage of flame development is carefully examined, a clear distinction on flame kernel growth between both raw and nanostructured spark plugs can be seen (Figure 6). In the case of the raw spark plug, the flame tends to develop in forward and lateral directions concurrently. However, the flame front in the nanostructured spark plug develops with higher growth rate in forward direction than lateral direction. As mentioned previously, the breakdown voltage in the nanostructured spark plug is lower than that of the raw one. This leads to a lower electric field strength in the nanostructured spark plug, which presents a lower energy for flame propagation in each direction into the combustible mixture. This may account for the lower growth rate in lateral direction compared to that in the nanostructured spark plug. Moreover, this may imply that the flame burning speed of flame front in early stage of propagation in forward direction for both spark plugs are relatively similar; however, the flame speed of the raw spark plug in lateral direction is higher than that of the nanostructured spark plugs.

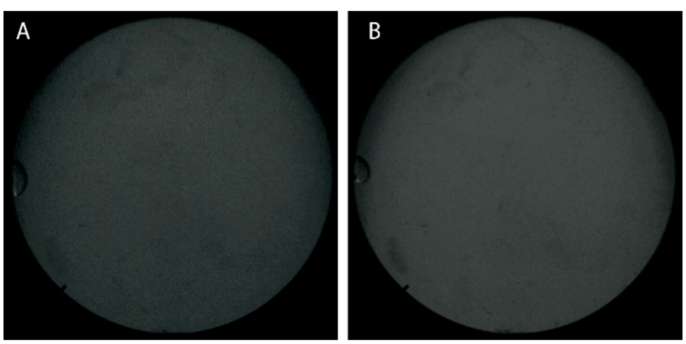

Figure 6. Flame kernel growth in early stage of premixed combustion at time frame of 3.9 ms for (A) Raw spark plug, (B) Nanostructured spark plug

Pressure and Temperature

Figure 7 shows the pressure history of methane-air premixed spark-ignited combustion for a range of lean equivalence ratio using each spark plug. The empirical results demonstrate that the lower equivalence ratios drive pressure to a lower range. In addition, the maximum pressure for the nanostructured spark plug is higher than that of the raw spark plug for all equivalence ratios. Maximum uncertainty of the pressure measurements is ±0.1 bar.

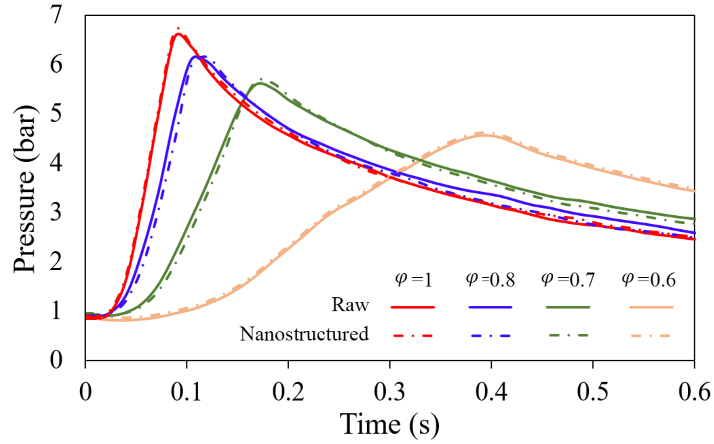

Figure 7. Comparison of pressure rise during the flame propagation for both spark plugs along equivalence ratio

An important portion of combustion process in internal combustion engines is related to the unburned gas temperature. The unburned gas temperature range of methane-air mixture is calculated with an assumption of an isentropic process, using the Equation 3. The indices 1 and 2 represent the primary and secondary thermodynamic states, respectively [35].

$$\frac{T_2}{T_1} = \left(\frac{P_2}{P_1}\right)^{\frac{\gamma-1}{\gamma}} \tag{3}$$

The temperature history of the unburned gas over time for both raw and nanostructured spark plugs in a range of lean equivalence ratios is plotted in Figure 8.

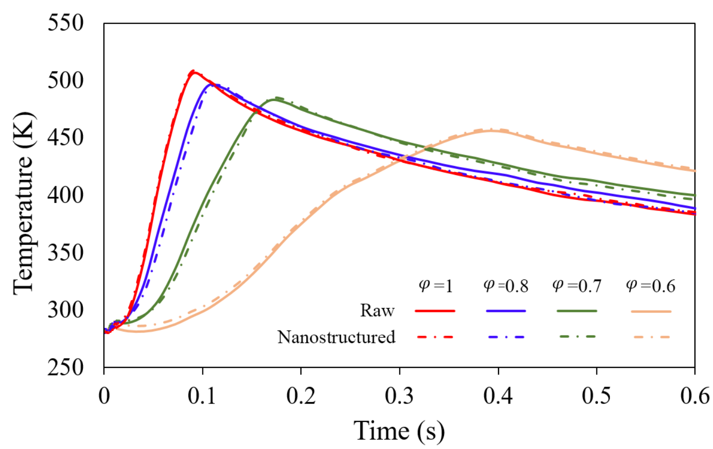

Figure 8. Comparison of temperature of unburnt mixture for both spark plugs along equivalence ratio

CONCLUSIONS

Two spark plugs with different electrode surface roughnesses were compared to investigate their effect on the flame kernel development and the lean flammability limit. The experiments indicate that the nanostructured spark plug extended the lean flammability limit of methane. The nanostructured spark plug has lower breakdown voltage and a lower electric field strength. This leads to a smaller flame growth rate in lateral direction in the early stage of ignition onset in comparison with the raw spark plug. The flame then develops outward through the chamber in a similar growth rate visually; however the flame front has higher instability in the raw spark plug when compared to the nanostructured spark plug.

NOMENCLATURE

A	Constant
n	Constant
P	Pressure
r	Compression ratio
R	Centerline average roughness
T	Temperature
V_{50}	50% breakdown voltage
γ	Specific heat ratio
η	Thermal efficiency

ACKNOWLEDGMENTS

The authors would like to recognize the University of Massachusetts Lowell for supporting this research, and to acknowledge Qinghua Zhu regarding his help on performing femtosecond laser pulses.

REFERENCES

[1] O. Askari, Z. Wang, K. Vien, M. Sirio, and H. Metghalchi, "On the flame stability and laminar burning speeds of syngas/O 2/He premixed flame," *Fuel,* vol. 190, pp. 90-103, 2017.

[2] J. Song, Z. Huang, X. Qiao, and W. Wang, "Performance of a controllable premixed combustion engine fueled with dimethyl ether," *Energy conversion and management,* vol. 45, no. 13-14, pp. 2223-2232, 2004.

[3] M. Morovatiyan, M. Shahsavan, and J. H. Mack, "Development of a Constant Volume Combustion Chamber for Material Synthesis," in *Eastern States Section of the Combustion Institute Spring Technical Meeting*, State College, PA, 2018.

[4] K. Seshadri *et al.*, "Experimental and kinetic modeling study of combustion of JP-8, its surrogates and components in laminar premixed flows," *Combustion Theory and Modelling,* vol. 15, no. 4, pp. 569-583, 2011.

[5] M. Shahsavan, M. Morovatiyan, and J. H. Mack, "A numerical investigation of hydrogen injection into noble gas working fluids," *International Journal of Hydrogen Energy,* vol. 43, no. 29, pp. 13575-13582, 2018.

[6] M. Shahsavan and J. H. Mack, "Mixedness Measurement in Gaseous Jet Injection," in *American Society for Engineering Education Northeast Section (ASEE-NE) Annual Conference*, Lowell, MA, 2017.

[7] A. Holley, Y. Dong, M. Andac, F. Egolfopoulos, and T. Edwards, "Ignition and extinction of non-premixed flames of single-component liquid hydrocarbons, jet fuels, and their surrogates," *Proceedings of the Combustion Institute,* vol. 31, no. 1, pp. 1205-1213, 2007.

[8] M. Shahsavan and J. H. Mack, "The Effect of Heavy Working Fluids on Hydrogen Combustion," in *10th US National Combustion Meeting*, College Park, MD, 2017.

[9] M. Shahsavan, M. Morovatiyan, and J. H. Mack, "The Influence of Mixedness on Ignition for Hydrogen Direct Injection in a Constant Volume Combustion Chamber," in *Eastern States Section of the Combustion Institute Spring Technical Meeting*, State College, PA, 2018.

[10] S. Liu, E. R. C. Clemente, T. Hu, and Y. Wei, "Study of spark ignition engine fueled with methanol/gasoline fuel blends," *Applied Thermal Engineering,* vol. 27, no. 11-12, pp. 1904-1910, 2007.

[11] D. Johnson, M. Darzi, C. Ulishney, M. Bade, and N. Zamani, "Methods to Improve Combustion Stability, Efficiency, and Power Density of a Small, Port-Injected, Spark-Ignited, Two-Stroke Natural Gas Engine," in *ASME 2017 Internal Combustion Engine Division Fall Technical Conference*, 2017, pp. V002T07A008-V002T07A008: American Society of Mechanical Engineers.

[12] M. R. Morovatiyan and V. Hosseini, "Development of a 3D CFD model to analyze gas exchange process into intake manifold of an iVVT engine," *The Journal of Engine Research,* vol. 36, no. 36, pp. 51-60, 2014.

[13] M. Shahsavan and J. H. Mack, "Numerical study of a boosted HCCI engine fueled with n-butanol and isobutanol," *Energy Conversion and Management,* vol. 157, pp. 28-40, 2018.

[14] S. Voshtani, M. Reyhanian, M. Ehteram, and V. Hosseini, "Investigating various effects of reformer gas enrichment on a natural gas-fueled HCCI combustion engine," *International Journal of Hydrogen Energy,* vol. 39, no. 34, pp. 19799-19809, 2014/11/20/ 2014.

[15] G. E. Bogin, J. H. Mack, and R. W. Dibble, "Homogeneous charge compression ignition (HCCI) engine," *SAE International Journal of Fuels and Lubricants,* vol. 2, no. 2009-01-1805, pp. 817-826, 2009.

[16] E. Ansari, K. Poorghasemi, B. K. Irdmousa, M. Shahbakhti, and J. Naber, "Efficiency and Emissions Mapping of a Light Duty Diesel-Natural Gas Engine Operating in Conventional Diesel and RCCI Modes," SAE Technical Paper 0148-7191, 2016.

[17] R. D. Reitz and G. Duraisamy, "Review of high efficiency and clean reactivity controlled compression ignition (RCCI) combustion in internal combustion engines," *Progress in Energy and Combustion Science,* vol. 46, pp. 12-71, 2015.

[18] G. T. Kalghatgi, "Spark ignition, early flame development and cyclic variation in IC engines," SAE Technical Paper 0148-7191, 1987.

[19] J. E. Dec, "Advanced compression-ignition engines—understanding the in-cylinder processes," *Proceedings of the combustion institute,* vol. 32, no. 2, pp. 2727-2742, 2009.

[20] L. M. Pickett, S. Kook, H. Persson, and Ö. Andersson, "Diesel fuel jet lift-off stabilization in the presence of laser-induced plasma ignition," *Proceedings of the Combustion Institute,* vol. 32, no. 2, pp. 2793-2800, 2009.

[21] B. Wolk, A. DeFilippo, J.-Y. Chen, R. Dibble, A. Nishiyama, and Y. Ikeda, "Enhancement of flame development by microwave-assisted spark ignition in constant volume combustion chamber," *Combustion and flame,* vol. 160, no. 7, pp. 1225-1234, 2013.

[22] J. S. Townsend, *Electricity in gases*. Рипол Классик, 1915.

[23] T. Badawy, X. Bao, and H. Xu, "Impact of spark plug gap on flame kernel propagation and engine performance," *Applied energy,* vol. 191, pp. 311-327, 2017.

[24] S. P. Bane, J. L. Ziegler, and J. E. Shepherd, "Investigation of the effect of electrode geometry on spark ignition," *Combustion and Flame,* vol. 162, no. 2, pp. 462-469, 2015.

[25] A. A. Abdel-Rehim, "Impact of spark plug number of ground electrodes on engine stability," *Ain Shams Engineering Journal,* vol. 4, no. 2, pp. 307-316, 2013.

[26] R. Moos, F. Rettig, A. Hürland, and C. Plog, "Temperature-independent resistive oxygen exhaust gas sensor for lean-burn engines in thick-film technology," *Sensors and Actuators B: Chemical,* vol. 93, no. 1, pp. 43-50, 2003/08/01/ 2003.

[27] M. Sjöberg and W. Zeng, "Combined effects of fuel and dilution type on efficiency gains of lean well-mixed DISI engine operation with enhanced ignition and intake heating for enabling mixed-mode combustion," *SAE International Journal of Engines,* vol. 9, no. 2016-01-0689, pp. 750-767, 2016.

[28] M. Perin and T. Achek, "Lean Burn Engines," SAE Technical Paper 0148-7191, 2013.

[29] M. Shen, J. E. Carey, C. H. Crouch, M. Kandyla, H. A. Stone, and E. Mazur, "High-density regular arrays of nanometer-scale rods formed on silicon surfaces via femtosecond laser irradiation in water," *Nano letters,* vol. 8, no. 7, pp. 2087-2091, 2008.

[30] S. Berger, "Onset or breakdown voltage reduction by electrode surface roughness in air and SF 6," *IEEE Transactions on Power Apparatus and Systems,* vol. 95, no. 4, pp. 1073-1079, 1976.

[31] S. Sato and K. Koyama, "Relationship between electrode surface roughness and impulse breakdown voltage in vacuum gap of Cu and Cu-Cr electrodes," *IEEE transactions on dielectrics and electrical insulation,* vol. 10, no. 4, pp. 576-582, 2003.

[32] K. L. Cashdollar, I. A. Zlochower, G. M. Green, R. A. Thomas, and M. Hertzberg, "Flammability of methane, propane, and hydrogen gases," *Journal of Loss Prevention in the Process Industries,* vol. 13, no. 3-5, pp. 327-340, 2000.

[33] Y. Shoshin and L. De Goey, "Experimental study of lean flammability limits of methane/hydrogen/air mixtures in tubes of different diameters," *Experimental Thermal and Fluid Science,* vol. 34, no. 3, pp. 373-380, 2010.

[34] S. R. Turns, *An introduction to combustion*. McGraw-hill New York, 1996.

[35] Z. Wang, M. Alswat, G. Yu, M. O. Allehaibi, and H. Metghalchi, "Flame structure and laminar burning speed of gas to liquid fuel air mixtures at moderate pressures and high temperatures," *Fuel,* vol. 209, pp. 529-537, 2017/12/01/ 2017.